The Array of Long-Baseline Antennas for Taking Radio Observations from the Sub-Antarctic

First Author[2], Second Author[3], Third Author[3] and Fourth Author[4]

[2]*Department, University Name, City, State ZIP/Zone, Country, fauthor@university.com*

[3]*Group, Company, Address, City, State ZIP/Zone, Country*

[4]*Group, Company, Address, City, State ZIP/Zone, Country, fauthor@company.com*

text to be overhauled later...

The low frequency radio astronomy has the highest potential in discovering the history of the Universe, this includes observations of the first stars and the mapping of dark ages. The Array of Long Baseline Antennas for Taking Radio Observations from the Sub-Antarctic (ALBATROS) is a new interferometric array. It consists of autonomous antenna stations that will map the low-frequency sky from Marion Island. One autonomous station was deployed in Marion Island in April 2019. The operating frequency range is 1.2 MHz to 81 MHz with baselines of ≈ 20 km. A two element pathfinder was deployed in Marion Island in April 2018.

Keywords: cosmology: observations; dark ages; instrumentation: interferometers

Open task for any/all: fix references, make a proper bibtex file

1. Introduction

Measurements of redshifted 21 cm emission of neutral hydrogen across a wide range of radio frequencies have the potential to elucidate the universe's history from the cosmic "dark ages" up to the formation of large-scale structures (see, e.g., (**?**Liu et al., 2013; Pober et al., 2014). The dark ages, which occurred after recombination and correspond to a period when the universe was filled with neutral hydrogen, are unexplored to date and represent one of the final observational frontiers in cosmology. This epoch contains a potential wealth of cosmological information (**?**Chen et al., 2019; Koopmans et al., 2019), but the required redshifted frequencies of $\lesssim 30$ MHz are exceptionally difficult to observe. The primary experimental challenges include Galactic foreground emission, ionospheric interference, and terrestrial radio-frequency interference (RFI).

Very few experiments have measured the radio sky at $\lesssim 30$ MHz. Comprehensive reviews exist elsewhere (**find a good reference**), and here, we highlight only a few specific examples. At the very lowest frequencies, the state of the art among ground-based measurements dates from the 1950s, when Reber and Ellis caught brief glimpses of the 2.1 MHz sky at $\sim 5°$ resolution, using an array of 192 dipoles (**?**George et al., 2018; Weiler et al., 1988). A few space-based missions have also performed measurements at similarly low frequency ranges; for example, the Radio Astronomy Explorer-2 operated at 0.025 MHz to 13 MHz with $\sim 10°$ resolution at 4.7 MHz (Alexander et al., 1975). Measurements with resolution finer than few-degree scales exist only at higher frequencies. For example, the Dominion Radio Astrophysical Observatory surveyed the northern sky at 22 MHz with 1.1° to 1.7° resolution (Roger et al., 1999), and most recently, the Owens Valley Long Wavelength Array mapped the sky with 15′ resolution between 36.528 MHz and 73.152 MHz (Eastwood et al., 2018). Although this experimental list is not comprehensive, it does illustrate
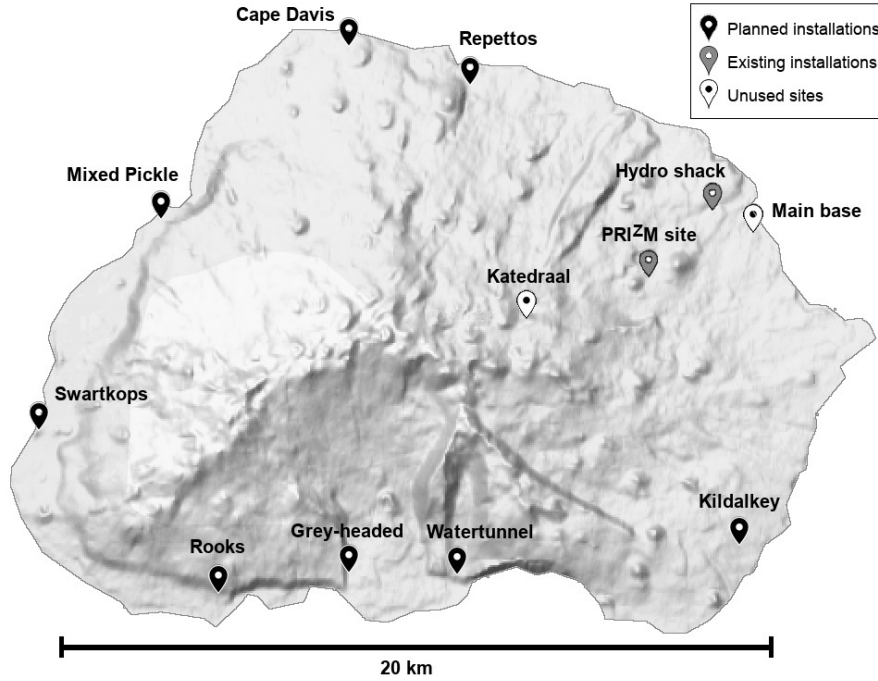
---

[2]Corresponding author.

Fig. 1: Map of Marion Island. The ALBATROS pathfinder antennas are currently installed at the PRI^{Z}M site and at the hydro shack. The black markers denote the eight coastal huts, which will be used for future ALBATROS antenna installations. The white markers denote other available infrastructure points that will not be used for antennas. **Add new synthesized beam figure (Jon)**

the dearth of information about the $\lesssim 30$ MHz sky and the lack of high resolution measurements at the lowest frequencies.

More text about the science case, including Galactic astrophysics (Jon? Jeff?)

Preliminary observations from Marion Island (Philip et al., 2019) suggest that despite the present-day RFI environment, low-frequency observations may still be accessible from carefully selected locations and with new technology developments. In this paper, we present the Array of Long Baseline Antennas for Taking Radio Observations from the Sub-Antarctic (ALBATROS), a new experimental effort that aims to map the low-frequency sky using an array of autonomous antenna stations. We describe the overall instrument design and preliminary measurements from engineering runs that were performed on Marion Island during 2018–2019.

2. ALBATROS overview

The primary requirements that drive the design for a low-frequency imaging experiment are 1) desired resolution, 2) low RFI, and 3) quiet ionospheric conditions. As a benchmark, an interferometer operating at 30 MHz requires order-of-magnitude baseline lengths of ~ 1 km to achieve a resolution of $\sim 1°$. This length scales inversely with frequency, and therefore ~ 10-km lengths are required at few-MHz frequencies in order to improve upon the resolutions achieved to date. The experiment installation site must be remote to keep RFI to a minimum, and polar or near-polar latitiudes generally have lower ionospheric plasma frequency cutoffs. **Add more ionosphere text here, plus IRI simulation fig/numbers (Jon)**

Marion Island is a research base that is located in the southern Indian Ocean at $46°54'45''$S, $37°44'37''$E and is operated by the South African National Antarctic Programme. The island lies roughly 2000 km from the nearest continental landmasses and has an exceptionally quiet RFI environment (Philip et al., 2019). As illustrated in Figure 1, Marion has an area of 335 km^2 and can therefore support antenna installations with > 10-km baseline lengths. The main Marion base is located on the northeast side of the island, and there are eight rest huts along the coast (Cape Davis, Grey-headed, Kildalkey, Mixed Pickle, Repettos,
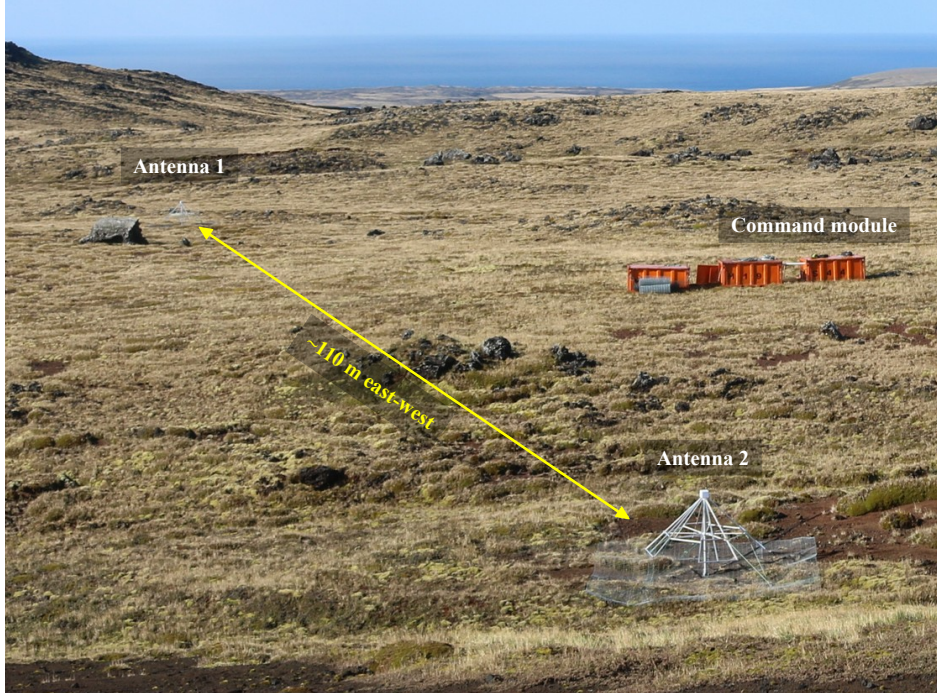
Fig. 2: The two-element, directly correlated ALBATROS pathfinder installed at the PRI$^{\rm Z}$M site. Two dual-polarization antennas are separated by roughly 110 m on an east–west baseline. Coaxial cables connect the antennas to a shipping container that houses the readout electronics and serves as the "command module." **Add FEE and backend sub-pics here? (HCC)**

Rooks, Swartkops, Watertunnel) and one in the interior (Katedraal) that can serve as existing infrastructure points for antenna installations. The planned ALBATROS installation sites include the coastal huts, but exclude the main base and Katedraal for RFI and accessibility reasons, respectively. Figure 1 also shows the locations of the ALBATROS pathfinder antennas that are currently installed at the PRI$^{\rm Z}$M site and at the hydro shack.

Using the eight coastal huts, the PRI$^{\rm Z}$M site, and the hydro shack as the nominal ALBATROS installation locations, the computed synthesized beam is as shown in Figure 1. The beam width at 5 MHz is roughly 8′, which represents over an order of magnitude improvement in resolution over other existing measurements. One of the challenges in constructing an interferometer array on Marion Island is that the rugged terrain precludes the possibility of directly cabling and correlating antennas across large distances. The final ALBATROS antenna stations will therefore operate *autonomously*, recording baseband data over extended periods of time for subsequent offline correlation. We have conducted two enginering runs: 1) a two-element, directly correlated pathfinder to qualitatively understand the sky signal, and 2) a single station to test the readout and power handling technology that are required for autonomous operation.

3. Two-element pathfinder

The first exploratory ALBATROS measurements were conducted with a two-element pathfinder that employed direct correlation (without autonomous operation). Figure 2 illustrates this pathfinder, which was installed at the PRI$^{\rm Z}$M site (46°53′13″S, 37°49′10.7″E) in April 2018. The system schematic is illustrated in Figure 3, and each of the subsystems is described in detail below.

3.1. *Antenna*

We employ two dual-polarization Long Wavelength Array (LWA) dipole antennas (Ellingson and Kramer , 2004). The LWA antennas have a long development history, are well characterized, and are simple to
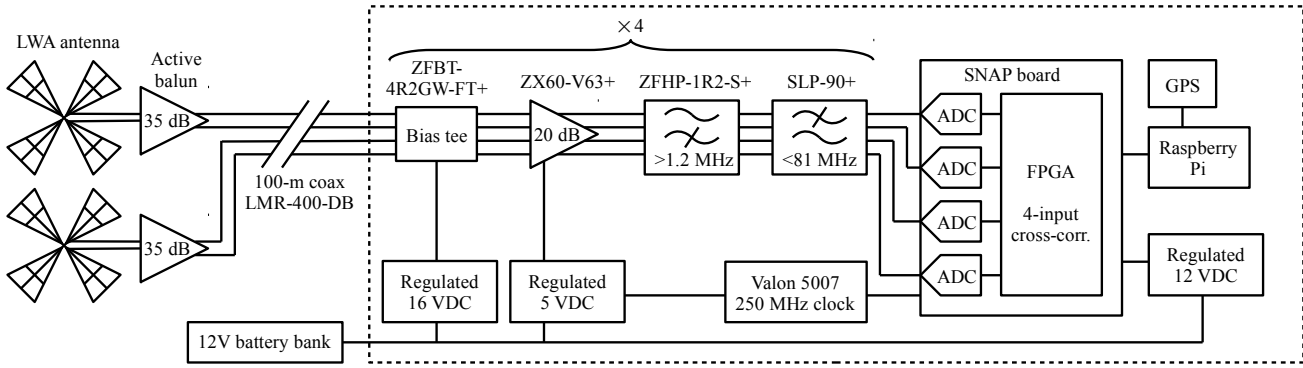
Fig. 3: Schematic for the two-element ALBATROS pathfinder. Signals from two dual-polarzation LWA antennas are amplified by front-end active baluns (**citation for FEE**), and 100-m coaxial cables connect the antennas to the back-end readout electronics, which are housed in a Faraday cage denoted by the dashed box. Each of the four antenna outputs is passed to a second-stage electronics chain consisting of a bias tee, amplifier, and high- and low-pass filters. The signals are digitized at 250 Msamp/s by a SNAP board, and the on-board FPGA is programmed with firmware to perform a full cross-correlation of all four inputs. A Raspberry Pi controls the SNAP board and also saves the computed spectra to an SD card. The clock signal is provided by a Valon frequency synthesizer. Power to the system is provided by a bank of 12 V batteries and several regulated voltage outputs.

install and physically robust. The antennas form an east–west baseline with a separation of 110 m, and the polarizations are aligned with the cardinal directions. Welded wire mesh screens, roughly 3 m on a side, are installed on the ground below the antennas.

ALL TEXT BELOW HERE NEEDS WORK

3.2. *Front-end active balun*

Tankiso, Eamon, Jeff?

The LWA active-balun front-end electronics (FEE) circuit uses a MiniCircuits GALI-74+ MMIC to amplify each dipole leg against ground, presenting each leg with a 50Ω impedance and providing a nominal gain of 25dB. The two GALI-74+ outputs are differenced using a passive 180° hybrid coupler. The coupler output is filtered by a ∼150MHz lowpass, and receives an additional 12dB of gain from a MiniCircuits GALI-6+ MMIC. This last amplifier drives the output signal onto a ∼100m 50Ω coaxial cable. Thus, neglecting mismatch loss between the dipoles (electrically small in the frequency range of interest) and the 100Ω input impedance, as well as the hybrid insertion loss (<1dB), the front-end electronics provide a gain of ∼37dB (Hicks et al., 2012).

Each FEE circuit is powered by 16V, fed on the coax through a bias tee.

3.3. *Back-end electronics*

Nivek, HCC?

The back-end readout electronics are housed in a Faraday cage that is located ∼100m away from the antennas to mitigate possible self-generated RFI. Each of the four antenna signals is passed to a second-stage electronics chain consisting of an amplifier (Minicircuits ZX60-V63+), and a pair of high- and low-pass filters (Minicircuits ZFHP-1R2+ and SLP-90+) that together bandlimit the signal to 1.2–81 MHz. The amplifier has a nominal gain of 20dB, and the HPF and LPF contribute nominal insertion losses of 0.2dB and 0.14dB respectively.
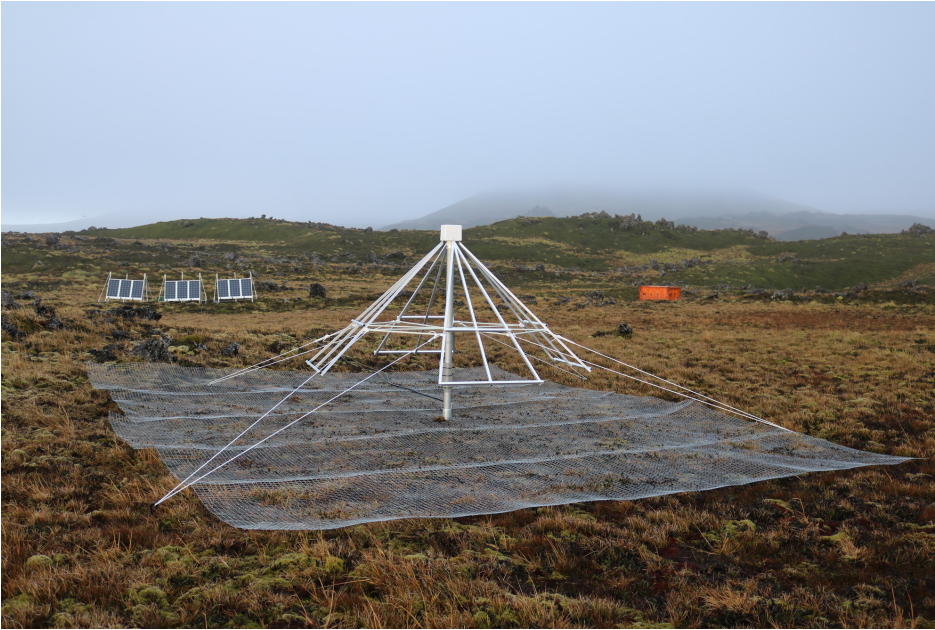
Fig. 4: Single autonomous station pathfinder installed at the hydro shack site. The system is powered by a bank of solar panels that are visible in the background. **Add command module and electronics glamor shots.**

A Xilinx Kintex[a] based Smart Network ADC Processor (SNAP) board (**citation for SNAP board?**), clocked by a Valon 5007 frequency synthesizer module, digitizes the RF signals at 250 Msamp/s. It calculates a full cross-correlation of the four inputs, producing four auto- and six cross-spectra as outputs, over 2048 channels spanning the frequency range 0 MHz - 125 MHz. (**details about SNAP board frequency transform?**) The SNAP board sends its output data via ethernet to a Raspberry Pi (**version? citation?**), which saves it to a hard drive.

3.4.   *Power*

In order to supply power to the whole two-element pathfinder sysytem, a bank of four 12 V, 200 A h batteries were wired in parallel. The Honda EU30is generator is used for charging the battery bank and the fuel is kept in one of the shipping containers at the PRI^{Z}M site. If the batteries are fully charged, the system can fully operate for approximately four days. The power from the battery bank is connected to the Faraday cage where the power regulation is performed. A DC/DC converter stabilises the 12 V from the battery bank and further supplies it to the auxiliary regulators that provide step down voltages to various components in the system.

3.5.   *Software and data acquisition*

Nivek?
Text goes here.

4.   Single autonomous station pathfinder

Nivek?

A single, autonomous station pathfinder was installed at the hydro shack (46°52.205′S, 37°50.612′E) in April 2019.

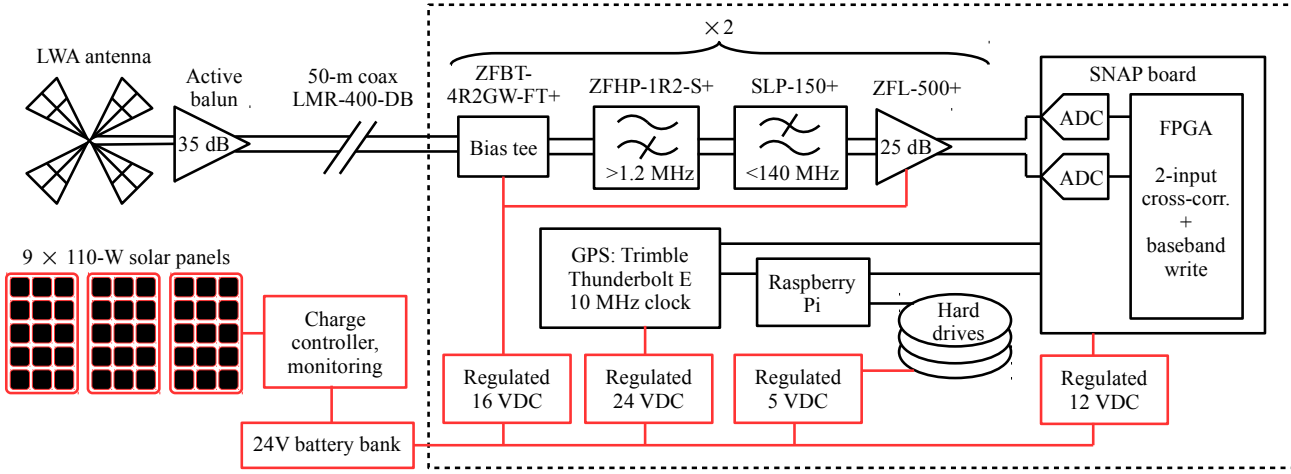[a]http://www.xilinx.com/products/silicon-devices/fpga/kintex-7.html

Fig. 5: Schematic for the single autonomous station pathfinder. Data and RF connections are outlined in black, and power connections are outlined in red. A dual-polarization LWA antenna, equipped with an active balun, is connected via 50-m coaxial cables to the back-end readout electronics, which are housed in a Faraday cage denoted by the dashed box. Each of the two antenna inputs is passed to a second-stage electronics chain consisting of a bias tee, high- and low-pass filters, and amplifier. The signals are digitized at 250 Msamp/s by a SNAP board, and the on-board FPGA is programmed with firmware that computes averaged auto- and cross-spectra, as well as channelized baseband. A Raspberry Pi controls the SNAP board and saves the data products to a combination of an SD card and external hard drives. Timing information is provided by a GPS-disciplined clock. Power to the system is provided solar panels that charges a 24-V battery bank, which is regulated down to several other output levels.

The final project (ALBATROS) will consist of autonomous antenna stations that will map the low frequency sky. Since these experiments are exploratory, they are taking steps towards achieving the future objective of probing the Dark Ages.The ALBATROS stations (huts) will be separated by baselines of ≈20 km as shown in **??**. The two-element interferomentric pathfinder is not yet operating autonomously, it uses the direct cross correlation technique whereas the yet to be ALBATROS will write the lowest 10 - 20 MHz baseband to disk then gets correlated afterwards. One ALBATROS fully autonomous station was deployed in Marion Island in April 2019 as shown in Figure 4.

The single antenna analog signal chain is shown in Figure 5. The components of the system are discussed in detail as per the block diagram illustrated in Figure 5. This analog signal chain is an illustration of how the first autonomous station is configured. There might be changes to the block diagram at a later stage should there be a need to revise it for the stations.

4.1.   *Readout electronics*

Nivek, Jon?

Text here about one-bit stuff, pushing baseband through the RPi3, clock requirements, data rates, etc.

4.2.   *Correlation*

While the basics of 1-bit correlation are well known in the limit where the signal level is much lower than the noise, ALBATROS may well be in the high-signal regime. We present the basics of 1-bit correlation here, and show that even in the high-signal limit, 1-bit correlation remains viable. The fundamental output of a 1-bit correlator for real data is $x_{ij} \equiv \left\langle \tilde{E}_i \tilde{E}_j \right\rangle$. $\tilde{E}_i$ is the quantized version of the underlying electric field E_i where $\tilde{E}_i = 1$ for $E_i > 0$ and $\tilde{E}_i = -1$ for $E_i < 0$. Note that complex data can be handled as the
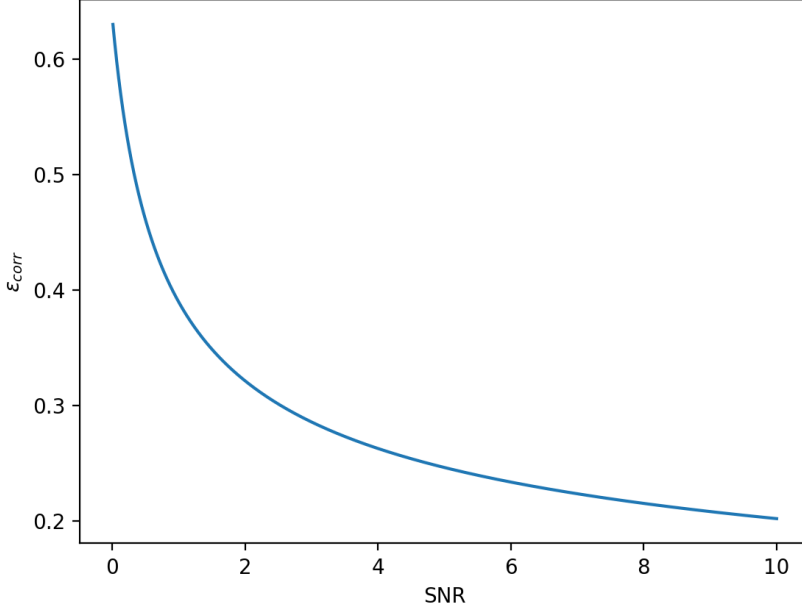
Fig. 6: Correlator efficiency ϵ_{corr} for a 1-bit correlator as a function of signal-to-noise ratio (SNR). To get the expected SNR from a 1-bit correlator, multiply the SNR derived from the radiometer equation by ϵ_{corr}. For low SNR, the efficiency is $2/\pi \sim 0.64$, and it drops monotonically as the SNR increases. The drop is relatively gentle, only changing by a factor of ~ 2 for SNR=2. For baseline separations of many wavelengths, the correlated component of the electric field is likely to be a small fraction of the total power, so ALBATROS is unlikely to lose more than a factor of ~ 2 by using 1-bit correlation.

combination of real components. This output is non-linear in the underlying true signal and noise levels, since the output saturates at unity for perfectly correlated electric fields. To get at the true sky signals, we will need to undo this nonlinearity (the so-called Van Vleck corrections). For a 2-level correlator, the expected output can be related to the true signals as follows (Van Vleck & Middleton, e.g. D'Addario):

$$\left\langle \sin(\frac{\pi}{2} x_{ij}) \right\rangle = \frac{V_{ij}}{\sqrt{V_{ij} + N_i}\sqrt{V_{ij} + N_j}} \tag{1}$$

where V_{ij} is the true visibility, and $V_{ij}+N_{i,j}$ is the total noise power measured by antennas i and j. Inverting this relation to get the true signal requires knowing the noise powers, which is not possible from the 1-bit data themselves. However, the SNAP board calculates these power levels on timescales of a few seconds, much faster than the power levels change, and so by combining the single-station power measurements with the cross-station cross correlation, we will be able to derive the true sky visibilities.

One might worry that at high signal levels, the saturation of the 1-bit cross correlation would lead to the noise exploding. In practice the rolloff in sensitivity is relatively mild, especially in the case of long baselines. It can be expressed in terms of the correlator efficiency ϵ_{corr}, which is defined to be the ratio of the measured signal-to-noise ratio to the ideal (infinite precision) SNR. As seen in Figure **??**, ϵ_{corr} only drops by a factor of ~ 2 as the signal power goes from 0 to a few times the noise power. We stress that the signal level is question is the part that correlates between the two antennas. In the case of long baselines (where long means the fringe spacing is small compared to the primary beam/antenna response pattern) that are not dominated by a single bright source, the signal power will always be smaller than the noise power, and so ϵ_{corr} is unlikely to drop below ~ 0.5[b].

---

[b]A quick estimate can be made by analogy to the behavior of dishes in the UV plane in the flat sky approximation. While all

4.3. *Solar power system*

Nivek, Tankiso, Eamon?

The power system of the ALBATROS-EGG uses generators to charge the batteries manually every once in a number of days. From the observation that has been made, the batteries take ≈ 2 days to discharge to a point where the system shuts down. Because of the weather conditions in Marion Island, an individual can sometimes be unable to go to the site to charge the batteries, which means that if the weather does not allow, the system can be shut down for a long period. Thus, a solar power system solution was introduced to the ALBATROS so that the system can continously run without having to be recharged manually and often.

The ALBATROS system is powered using 24 V power which is stored and provided by two series-connected 12 V deep-cycle lead-acid storage batteries. This power comes from the solar panel array consisting of nine flexible solar panels, each with a standard test condition capacity of 110 W. The solar panel type is SunPower SPE-E-Flex-110. The panels are grouped in three parallel connected strings of three panels. Each group of three is mounted on its own structure. The panels include diodes to bypass shaded or defective cells, and also to prevent backwards current flow in the event an entire string of three panels is not illuminated while the others are producing power.

The Victron BlueSolar MPPT 50|35 charge controller outputs a data packet every second, to an Arduino based data logger, which controls a switch that determines when the rest of the system runs. It also converts the solar panel voltage to 24 V to control the battery charging. The observed parameters are then stored to the raspberry pi.

5.   Preliminary observations

NEED UPDATED AND NEW PLOTS, NEED VOLUNTEERS FOR THIS:

- **Improved waterfall plots from 2-element pathfinder**
- **Plot showing that the solar power works (sort of)**
- **Some sort of...data...plot for the autonomous station. Can we say anything about baseband performance?**

Figure 7 and Figure 8 shows the initial results from the two interferometric array. These results are an encouraging factor to proceed with the development of the autonomous stations.Figure 7 shows the raw ALBATROS-EGG autospectra which where the waterfall plot was taken from one polarization (pol0) over an interval of 3 days. The Galaxy rising/setting is clearly visible in the structure. There are also ripples in frequency because of uncalibrated data, and the ripples arise from reflections in the cables. There is a qualitative difference between daytime and nighttime data and this shows that the contamination from shortwave radio drops off significantly at night, when the ionosphere becomes quieter.

Figure 8 shows the first fringes that were detected by the the ALBATROS-EGG. It is dinstictly visible from Figure 8 that fringes show recurrent structure down to a frequency of as low as 10 MHz without data processing or data cuts.

Acknowledgments

References

Alexander, J. K., Kaiser, M. L., Novaco, J. C., et al. 1975, *aap*, **40**, 365

---

power in the UV plane (plus any system noise) goes into an individual antenna's electric field, the correlated part only has contribution from the area in the UV plane within the width of the UV-space primary beam of the UV-space coordinate. If the sky can be described as a Gaussian random field, in the most pessimistic case this is roughly the aperture filling factor of the antenna pair. In our case, where the antennas are approximately dipolar, the filling factor will be the square of the wavelength over the baseline length. As long as the baselines are several wavelengths or longer, the correlated power will be small, and the correlator efficiency will be close to the ideal 1-bit value of $\frac{2}{\pi}$.
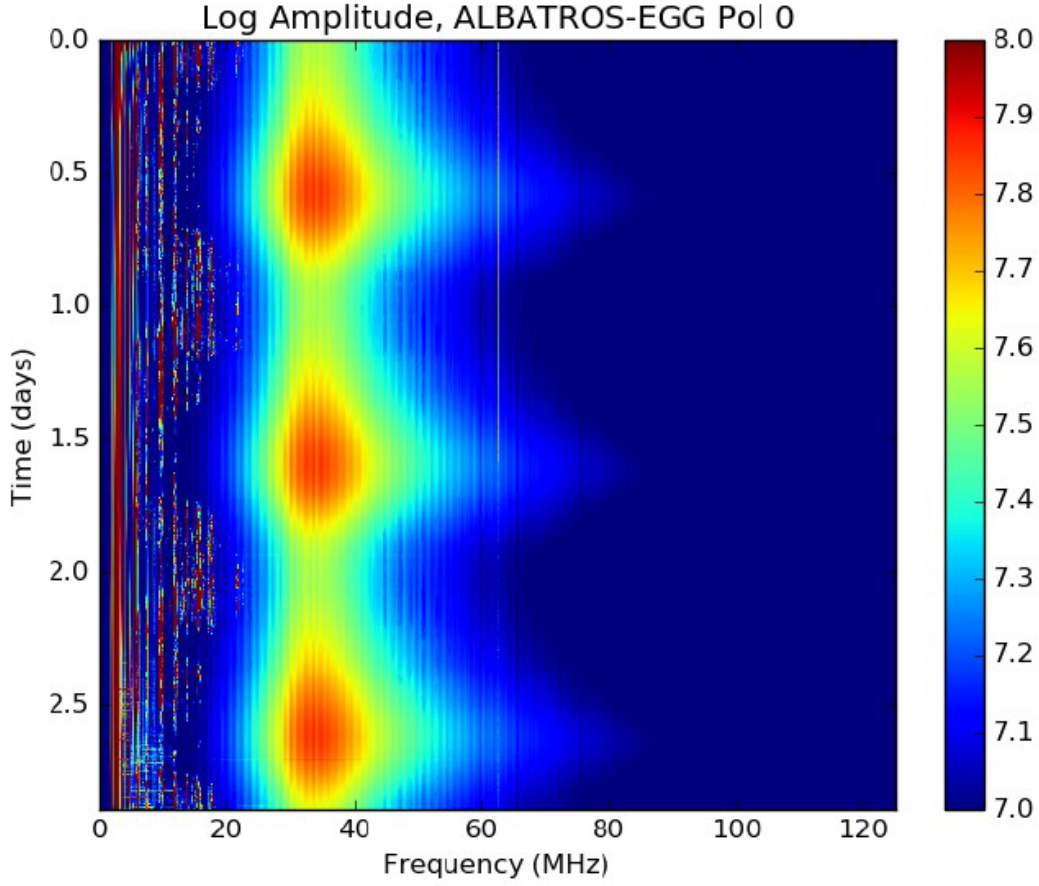
Fig. 7: Raw ALBATROS-EGG Autospectra

Chen, X., Burns, J., Koopmans, L., *et al.* [2019], arXiv e-prints, arXiv:1907.10853

Eastwood, M. W., Anderson, M. M., Monroe, R. M., et al. 2018, *aj*, **156**, 32

Ellingson, S. W., Kramer, W. T. 2004, *Long Wavelength Array Memo (28)*

George, M., Orchiston, W., Wielebinsk, R., *et al.* [2018], Journal of Astronomical History and Heritage, **21**, 37

Hicks, B. C., Paravastu-Dalal, N., Stewart, K. P., et al. 2012, *pasp*, **124**, 1090

Koopmans, L., Barkana, R., Bentum, M., *et al.* [2019], arXiv e-prints, arXiv:1908.04296

Liu, A., Pritchard, J. R., Tegmark, M., *et al.* [2013], **87**, 043002

Philip, L., Abdurashidova, Z., Chiang, H. C., *et al.* [2019], Journal of Astronomical Instrumentation, **8**, 19500

Pober, J. C., Liu, A., Dillon, J. S., *et al.* [2014], **782**, 66

Ray, P. S., Ellingson, S. W., Fisher R., *et al.* [2006] *Long Wavelength Array Memo (35)*

Roger, R. S., Costain, C. H., Landecker, T. L., et al. 1999, *aaps*, **137**, 7

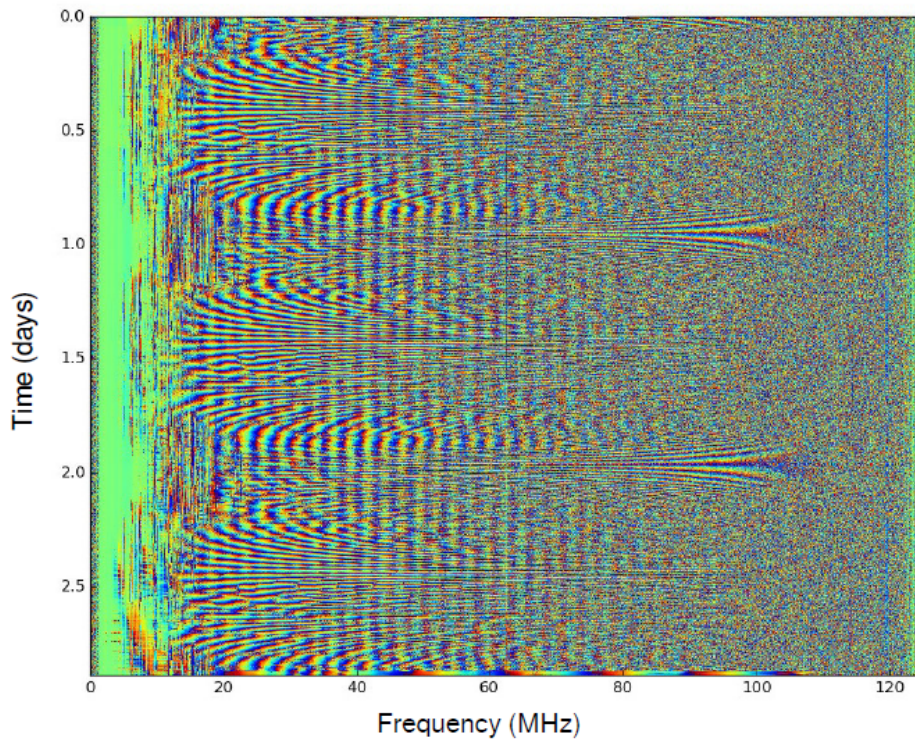Weiler, K. W., Johnston, K. J., Simon, R. S., *et al.* [1988], *aap*, **195**, 372

Fig. 8: First Fringes from ALBATROS-EGG